Journal of Physiology (1992), **453**, *pp.* 503–523
With 11 *figures*
Printed in Great Britain

PROPERTIES OF THE PACEMAKER CURRENT (I_f) IN LATENT PACEMAKER CELLS ISOLATED FROM CAT RIGHT ATRIUM

BY ZHENGFENG ZHOU AND STEPHEN L. LIPSIUS

From the Loyola University of Chicago, Stritch School of Medicine, Department of Physiology, Maywood, IL 60153, USA

(*Received 17 June 1991*)

SUMMARY

1. Single latent pacemaker cells were isolated from the Eustachian ridge of cat right atrium using Langendorff perfusion and enzyme dispersion techniques. Whole-cell patch-clamp techniques were used to study the hyperpolarization-activated inward current (I_f).

2. All cells studied beat rhythmically. Pacemaker activity was recorded in the voltage range -68 ± 1 to -54 ± 2 mV and its cycle length was 901 ± 67 ms (72 ± 5 beats min^{-1}) at 34–36 °C. Cells were elongated with tapered ends, and appeared bent or crinkled without obvious striations. Mean cell diameter and length were $7{\cdot}4 \pm 0{\cdot}5$ μm and $93{\cdot}1 \pm 5{\cdot}9$ μm, respectively ($n = 15$). Input resistance and total membrane capacitance were $2{\cdot}2 \pm 0{\cdot}2$ GΩ and $27{\cdot}8 \pm 3{\cdot}1$ pF, respectively.

3. Hyperpolarizing clamp steps more negative than -50 mV elicited a time-dependent increasing inward current that was maximally activated at -120 mV. Activation of I_f was well within the pacemaker voltage range. Half-maximal activation voltage and slope factor were calculated, using a Boltzmann function, to be $-80{\cdot}5$ mV and 8·4, respectively.

4. The fully activated current–voltage (I–V) relationship was approximately linear at voltages more negative than -30 mV and showed outward rectification at more positive voltages. The reversal potential of I_f was -26 mV and the fully activated conductance was $1{\cdot}75 \pm 0{\cdot}14$ nS ($n = 21$). Caesium (2 mM) blocked I_f at voltages more negative than the reversal potential. Reducing extracellular Na^+ or K^+ shifted the reversal potential more negative, and increasing extracellular K^+ exerted the opposite effect. Reducing extracellular Na^+ decreased I_f amplitude and the slope of the fully activated I–V relationship, and elevated extracellular K^+ increased I_f amplitude and the slope of the fully activated I–V relationship.

5. Some pacemaker cells exhibited a short delay in the onset of I_f activation whereas other pacemaker cells exhibited little, if any, delay in activation. I_f currents exhibiting no delay in activation were best fitted by a single exponential function with a mean time constant of $3{\cdot}20 \pm 1{\cdot}03$ s at -70 mV ($n = 4$).

6. A nystatin-permeabilized patch recording method was used to record spontaneous pacemaker action potentials and I_f from the same pacemaker cell. Caesium (2 mM) inhibited I_f by more than 90% (at -70 mV), and decreased the slope of diastolic depolarization, resulting in a 48 ± 5% decrease in spontaneous rate.

MS 9484
17
PHY 453

7. The present experiments demonstrate the isolation of Ca^{2+}-tolerant latent pacemaker cells from the Eustachian ridge of cat right atrium. Latent atrial pacemakers appear morphologically and electrophysiologically similar, though not identical, to pacemaker cells isolated from sino-atrial (SA) node. The hyperpolarization-activated inward current, I_f is activated within the latent pacemaker voltage range and contributes significantly to latent pacemaker function. The relatively long time course and small amplitude of I_f activation may explain, in part, the relatively long spontaneous cycle length of latent atrial pacemakers.

INTRODUCTION

There is extensive evidence that latent (subsidiary) atrial pacemakers are located within specific regions of the mammalian right atrium (Sealy, Bache, Seaber & Bhattacharga, 1973; Jones, Euler, Hardie, Randall & Brynjolfsson, 1978; Randall, Talano, Kaye, Euler, Jones & Brynjolfsson, 1978; Euler, Jones, Gunnar, Loeb, Murdock & Randall, 1979; Boineau, Schuessler, Hackel, Miller, Brockus & Wylds, 1980; Rozanski, Lipsius & Randall, 1983; Rozanski & Lipsius, 1985; Rubenstein, Fox, McNulty & Lipsius, 1987; Rubenstein & Lipsius, 1989). These pacemakers may become dominant in the case of sino-atrial node (SA node) dysfunction, or may act as ectopic foci to generate dysrhythmias. Both *in vivo* and *in vitro* experiments have shown that following surgical excision (Jones *et al.* 1978; Randall *et al.* 1978; Euler *et al.* 1979), exclusion (Sealy *et al.* 1973) or suppression (Rozanski *et al.* 1983; Rozanski & Lipsius, 1985) of the SA node, the site that assumes pacemaker activity is consistently located in the caudal region of the right atrium. Further *in vitro* experiments have localized this latent pacemaker activity to the Eustachian ridge (Rozanski & Lipsius, 1985; Rubenstein *et al.* 1987; Rubenstein & Lipsius, 1989). The Eustachian ridge is a caudal extension of the crista terminalis that lies within the distribution of the posterior internodal pathway, and runs close to the opening of the inferior vena cava (Sherf & James, 1979). Morphological studies have shown that cells thought to be responsible for SA node pacemaker activity, i.e. P cells (James, Sherf, Fine & Morales, 1966; Taylor, D'Agrosa & Burns, 1978), are found in specific extranodal regions of the right atrium. Sherf & James (1979) reported that P cells are found in the Eustachian ridge and Bachmann's bundle of human and canine hearts. In addition, P cells within the Eustachian ridge have been correlated with pacemaker activity, and are ultrastructurally similar to those found in SA node (Rubenstein *et al.* 1987). These studies indicate that the Eustachian ridge is a functionally important site of latent pacemaker activity, and that this activity may be generated by pacemaker cells similar to those found in SA node.

Voltage-clamp studies of a variety of cardiac pacemaker tissues have recorded the so-called pacemaker current, i_h (Yanagihara & Irisawa, 1980) or I_f (Brown & DiFrancesco, 1980; DiFrancesco & Ojeda, 1980; DiFrancesco, 1981*a*, *b*; Callewaert, Carmeliet & Vereecke,, 1984; Nakayama, Kurachi, Noma & Irisawa, 1984; DiFrancesco, Ferroni, Mazzanti & Tromba, 1986; Nathan, 1986; Bois & Lenfant, 1990; van Ginneken & Giles, 1991). This is a time-dependent inward current that is activated by hyperpolarization to voltages more negative than approximately -50 mV and blocked by low concentrations of caesium. Although I_f has been extensively studied in SA node pacemaker tissues, its relative contribution to

primary pacemaker activity has been debated (Noma, Morad & Irisawa, 1983; Hagiwara & Irisawa, 1989). However, recent work (Denyer & Brown, 1990*b*; DiFrancesco, 1991; van Ginneken & Giles, 1991) has provided additional evidence supporting a significant role for I_f in primary pacemaker function.

Because latent pacemakers exhibit a somewhat more negative pacemaker voltage range than SA node cells, I_f may contribute more to latent than primary pacemaker activity (Noble, 1985; Anumonwo, Delmar & Jalife, 1990). At the present time, however, little is known about the role of I_f in right atrial latent pacemaker function. The contribution of I_f to latent atrial pacemaker activity was suggested initially by experiments in multicellular Eustachian ridge preparations in which 1–2 mM-caesium decreased the slope of diastolic depolarization and increased pacemaker cycle length (Rubenstein & Lipsius, 1989). Single myocytes isolated from cat right atrium that exhibited pacemaker activity also exhibited a caesium-sensitive I_f current (Wu, Vereecke, Carmeliet & Lipsius, 1991). However, it was not possible to determine the origin of these latent pacemakers within the right atrium. In addition, a detailed analysis of I_f in right atrial latent pacemakers is lacking.

In the present study, we sought to isolate single latent pacemaker cells specifically from the Eustachian ridge of cat right atrium, and systematically analyse the properties of I_f using whole-cell patch-clamp techniques. Our results indicate that latent atrial pacemaker cells are morphologically and electrophysiologically similar, though not identical, to SA node pacemakers, and that I_f plays a significant role in right atrial latent pacemaker function.

An abstract of this work has been published (Zhou & Lipsius, 1990).

METHODS

Isolation procedure

Thirty-one adult cats of either sex, weighing 1·5–3·5 kg, were anesthetized with sodium pentobarbitone (30–50 mg kg^{-1}, I.P.) and injected with heparin (500 units kg^{-1}, I.P.). Atrial myocytes were isolated using a method similar to that described previously (Wu *et al.* 1991). Briefly, after a mid-sternal thoracotomy the heart was quickly removed and mounted on a Langendorff perfusion apparatus. The heart was perfused for 5 min with a bicarbonate-buffered Tyrode solution containing (mM): NaCl, 137; KCl, 5·4; $CaCl_2$, 1·8; $MgCl_2$, 1·0; $NaHCO_3$, 12; NaH_2PO_4, 0·6; glucose, 11; and bubbled with 95% O_2–5% CO_2 to yield pH 7·4. This was followed by a 5 min perfusion with a nominally Ca^{2+}-free Tyrode solution, and a final perfusion for 30–40 min with a Tyrode solution containing 36 μM-Ca^{2+}, 0·1% albumin and 0·07% collagenase (Worthington Biochemical, type II). The enzyme perfusate was recirculated with a pump. During the enzyme perfusion phase, 50 μl of Ca^{2+} stock solution (54 mM) was added to the perfusate every 8 min to yield a final Ca^{2+} concentration of approximately 150 μM. After the enzyme perfusion, both atria were removed from the heart. The right atrium was opened to expose the endocardium and the region of the Eustachian ridge ($\approx 6 \times 3$ mm) was excised. This tissue was cut into two pieces and incubated in fresh enzyme solution for 30–40 min at 36 °C while being agitated in a shaking water bath. In addition to collagenase, the incubation media contained 0·01% protease and/or 0·1% elastase. The tissue suspension was filtered through a nylon mesh (210 μm) using Tyrode solution containing 200 μM-Ca^{2+} and 0·05% albumin. After the cells settled for about 30 min the solution was suctioned off and gradually replaced with a HEPES-buffered solution containing (mM): NaCl, 137; KCl, 5·4; $MgCl_2$, 1·0; $CaCl_2$, 1·8; HEPES, 5; glucose, 11; and titrated with NaOH to pH 7·4. Cells were stored in this solution at room temperature until use.

Drugs

When appropriate the following compounds were used to block other currents that might interfere with the analysis of I_f: 3 mM-nickel to block slow inward Ca^{2+} currents and Na^+–Ca^{2+} exchange current (Kimura, Miyamae & Noma, 1987), 3 mM-barium to block K^+ currents (Glitsch,

Pusch, Schumacher & Verdonck, 1982; Osterrieder, Yang & Trautwein, 1982), and 2 mM-4-aminopyridine to block transient outward current (Kenyon & Gibbons, 1979). In some experiments, 20 μM-TTX was used to block fast Na^+ current. When extracellular Na^+ concentration was reduced NaCl was replaced with equimolar quantities of Tris-HCl. Extracellular K^+ concentrations were changed without compensation for total osmolarity.

Patch-clamp recording techniques

Cells used for study were transferred to a small tissue bath (0·5 ml) mounted on the stage of an inverted microscope (Nikon Diaphot), and were superfused with prewarmed HEPES-buffered Tyrode solution at a rate of 1–3 ml min^{-1}. All experiments were performed at a temperature of 34–36 °C. Action potentials and ionic currents were recorded in the whole-cell configuration using suction pipettes, as described by Hamill, Marty, Neher, Sakmann & Sigworth, (1981). The pipettes had inner diameters of 1–1·5 μm and when filled with the internal pipette solution had resistances of 3–6 MΩ. Standard internal pipette solutions contained (mM): potassium glutamate, 120; KCl, 20; $MgCl_2$, 1·0; EGTA, 1·0; Na_2ATP, 4; HEPES, 5; and titrated with KOH to pH 7·2. All recordings were corrected for liquid junction potentials between internal pipette and bath solutions (about 10 mV). Once a suction pipette made a gigaohm seal with the cell membrane additional suction was applied to rupture the membrane patch. In some experiments, signals were recorded without rupturing the membrane patch by adding 100–150 μg ml^{-1} nystatin to the internal pipette solution to permeabilize the membrane patch (Horn & Marty, 1988). The nystatin recording method was not used in the voltage-clamp analysis of I_f because this method does not buffer Ca^{2+} transients that interfere with the analysis. In some experiments, pacemaker cycle length was measured without using a patch electrode. This was accomplished by monitoring contractile events associated with pacemaker activity with a video-based edge detector (Crescent Electronics). Cycle length was determined by averaging ten consecutive cycles in cells exhibiting regular pacemaker activity. An Axoclamp-2A amplifier was used to record action potentials (bridge mode) and ionic currents (discontinuous single electrode voltage-clamp mode). In the voltage-clamp mode the amplifier sample rate was 10–12 kHz. Computer software (Pclamp program) was used to generate voltage-clamp protocols as well as acquire and analyse voltage and current signals. Voltage and current traces were sampled by a 12-bit resolution A/D converter (Tecmar Labmaster) using a computer. Data were stored on hard disc and videotaped for later analysis.

Measurements and data analysis

The input resistance was determined from the voltage response to a constant hyperpolarizing current pulse of 10 pA delivered during the diastolic interval. The membrane capacitance was measured by delivering a ramp voltage clamp pulse ($dV/dt = 5$ V s^{-1}) and dividing the half-amplitude of current jump at the turning point of the ramp pulse by the slope of the ramp (Kimura *et al.* 1987). When appropriate, currents are normalized in reference to total membrane capacitance of each cell to yield current density (pA pF^{-1}). Data are presented as means ± standard error of the mean (S.E.M.). Student's *t* test was used for statistical analysis and data with P values $< 0·05$ were considered statistically significant.

RESULTS

Morphology and passive membrane properties

Figure 1 shows two typical latent atrial pacemaker cells isolated from the Eustachian ridge of the cat right atrium. Both cells were beating spontaneously in normal Tyrode solution containing 1·8 mM-Ca^{2+}. Pacemaker activity was associated with spontaneous contractions, characterized by distinct twitches that were synchronous throughout the cell. In general, approximately 5–20% of the cells isolated in an individual experiment exhibited spontaneous, rhythmic pacemaker activity. The mean spontaneous beating rate of pacemaker cells (monitored by video-based edge detection) was 69 ± 4 beats min^{-1} ($n = 15$). Pacemaker cells were elongated with tapered ends, and appeared somewhat bent or crinkled, without obvious striations. Pacemaker cells exhibited a mean diameter and length of 7·4 ± 0·5

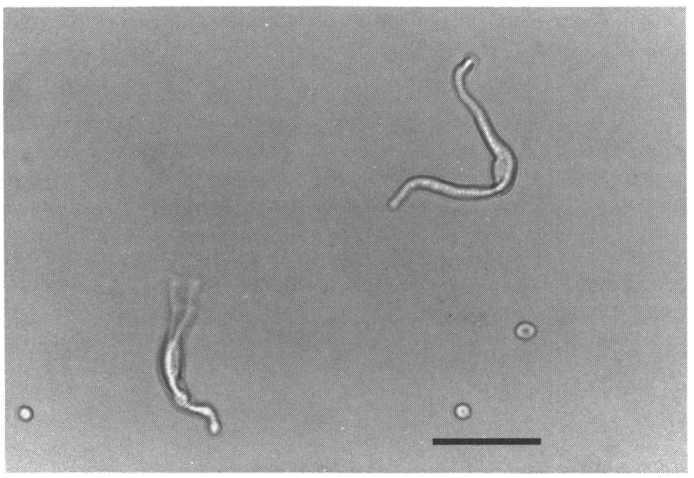

Fig. 1. Two typical latent pacemaker cells isolated from the Eustachian ridge of cat right atrium. Both cells exhibited rhythmic spontaneous activity. Cell at lower left was photographed during contractile event. Calibration bar = 40 μm.

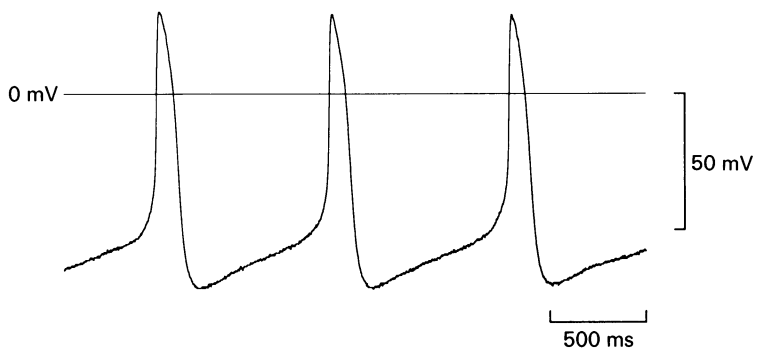

Fig. 2. Pacemaker action potentials recorded from a single spontaneously active cell isolated from Eustachian ridge of cat right atrium.

and 93·1 $\pm$ 5·9 μm, respectively (n = 15). The mean total membrane capacitance and input resistance were 27·8 $\pm$ 3·1 pF (n = 19) and 2·2 $\pm$ 0·2 GΩ (n = 21), respectively. These morphological and passive membrane properties are similar to those found in SA node pacemaker cells (Denyer & Brown, 1987, 1990*a*; Belardinelli, Giles & West, 1988) and pacemaker cells from cat right atrium (Wu *et al.* 1991).

Pacemaker action potential characteristics

Figure 2 shows typical pacemaker action potentials recorded from a latent atrial pacemaker cell using a ruptured-patch whole-cell recording configuration. These action potentials exhibited a relatively slow rate of rise (< 10 V s^{-1}) and a pacemaker voltage range between -71 and -54 mV. In some cells the diastolic slope exhibited two phases; an initial steeper slope followed by a more gradual slope. Table 1 summarizes the action potential parameters obtained from single latent pacemaker

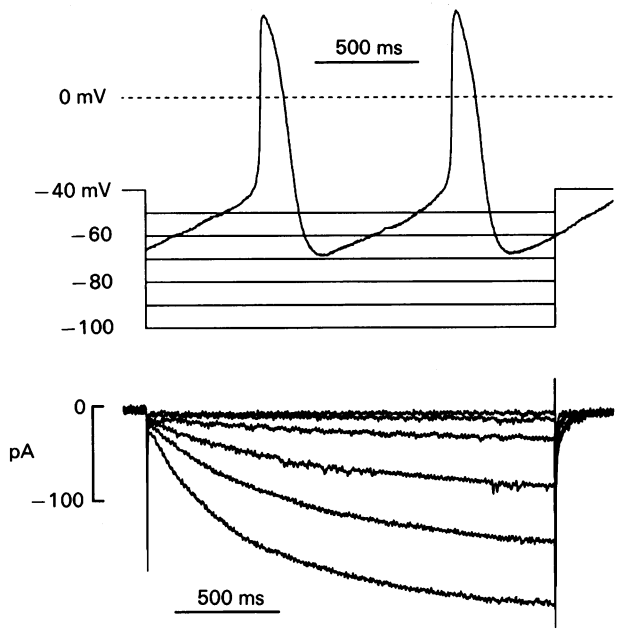

Fig. 3. Action potentials (top) and membrane currents (bottom) recorded from a single latent atrial pacemaker cell. Top panel shows voltage-clamp protocols superimposed on spontaneous action potentials. Bottom panel shows the recording of I_f in the same cell. Membrane currents were elicited by hyperpolarization clamp pulses between −50 and −100 mV from a holding potential of −40 mV.

TABLE 1. Spontaneous action potential parameters in latent pacemaker cells

Parameter	Mean	±S.E.M.
Maximum diastolic potential (mV)	−68·2	1·2
Overshoot (mV)	27·5	1·5
Amplitude (mV)	95·7	1·8
Take-off potential (mV)	−54·4	1·5
Duration (60%) (ms)	141·1	11·2
Upstroke velocity (V s^{-1})	6·5	1·6
Slope of diastolic depolarization (mV s^{-1})	35·4	3·4
Spontaneous cycle length (ms)	900·7	66·8

cells ($n = 15$). As expected for latent pacemakers the slope of diastolic depolarization was small (35 mV s^{-1}) and the spontaneous cycle length was long (901 ± 67 ms) compared with those reported in SA node (Nakayama *et al.* 1984; DiFrancesco, 1991; van Ginneken & Giles, 1991). The maximum diastolic potential was about −68 mV. Although spontaneous action potentials could be recorded for as long as 20 min in some cells, usually spontaneous activity gradually slowed and finally stopped within 5 min of rupturing the membrane patch. Similar results have been reported in rabbit SA node (Nakayama *et al.* 1984; DiFrancesco *et al.* 1986) and frog sinus venosus pacemaker cells (Bois & Lenfant, 1990). Action potentials were, therefore, recorded immediately after breaking the membrane. In later experiments we used a nystatin-

permeabilized patch method to record pacemaker action potentials for more than 30 min without run-down (see Fig. 11). Action potentials recorded from single latent pacemaker cells were comparable to those obtained from pacemakers in multicellular Eustachian ridge preparations (Rubenstein *et al.* 1987; Rubenstein & Lipsius, 1989).

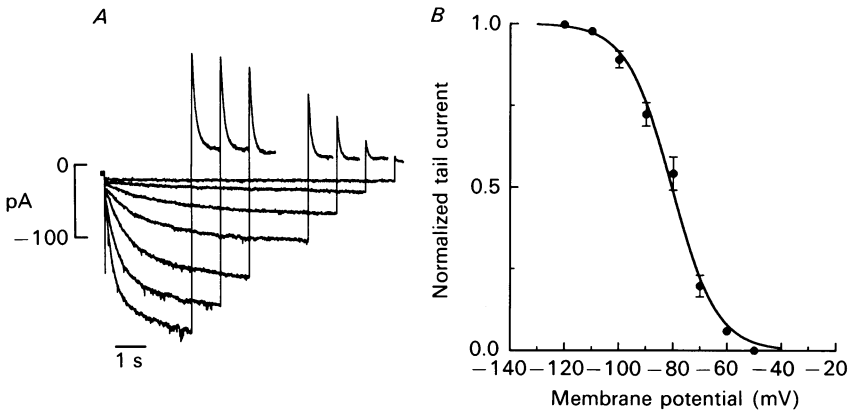

Fig. 4. Activation curve of I_f. *A*, selected membrane currents used to determine the voltage dependence of I_f activation curve. The cell was held at −40 mV and hyperpolarized between −60 and −120 mV for 3–10 s and then clamped to +10 mV for 1 s. *B*, tail current amplitudes are normalized with respect to maximal tail current amplitude and plotted against the voltage imposed during hyperpolarization. Data points (●) are means ± S.E.M. obtained from four cells. The activation curve (smooth curve) was obtained by fitting the data with a Boltzmann equation: $q_\infty = \{1+\exp[(V_t - V_{0.5})/k]\}^{-1}$, where q_∞ = steady-state activation variable, determined as the ratio of the tail current amplitude to maximal tail current amplitude, V_t = hyperpolarizing test voltage, $V_{0.5}$ is half-maximal voltage and k is the slope factor. External solution contained 3 mM-Ni^{2+}, 3 mM-Ba^{2+} and 2 mM-4-aminopyridine.

Hyperpolarization-activated current, I_f

Figure 3 shows an experiment where both action potentials and ionic currents were recorded from a single latent atrial pacemaker cell. Action potentials exhibited a pacemaker potential with a voltage range between −69 and −45 mV. Following these voltage recordings, the cell was clamped at a holding potential of −40 mV and hyperpolarized in 10 mV increments. Hyperpolarization elicited a relatively small initial inward current, indicating that the inward rectifying current, I_{K1} was very small or absent in these cells (Wu *et al.* 1991). This was later confirmed by the fact that barium had no significant affect on this initial inward current (Fig. 4). Over time an inward current developed that increased at more negative voltages. This time- and voltage-dependent inward current corresponds to the hyperpolarization-activated current, I_f found in SA node (Nakayama *et al.* 1984; DiFrancesco *et al.* 1986; Denyer & Brown, 1990*a*; van Ginneken & Giles, 1991), Purkinje (DiFrancesco, 1981*a*, *b*; Callewaert *et al.* 1984) and other cardiac pacemaker cells (Bois & Lenfant, 1990; Anumonwo *et al.* 1990; Wu *et al.* 1991). Of the 213 cells selected for study, 201 cells (94 %) exhibited I_f in response to hyperpolarization. This experiment shows that the threshold for I_f activation was between −50 and −60 mV, well within the pacemaker voltage range. It should also be noted that I_f amplitude varied among

different pacemaker cells. Typically, maximum I_f amplitude elicited at −120 mV ranged from 100 to 300 pA and was no greater than 400 pA. These values are considerably smaller than that reported in SA node (DiFrancesco *et al.* 1986; van Ginneken & Giles, 1991), where I_f amplitudes of more than 1000 pA are not

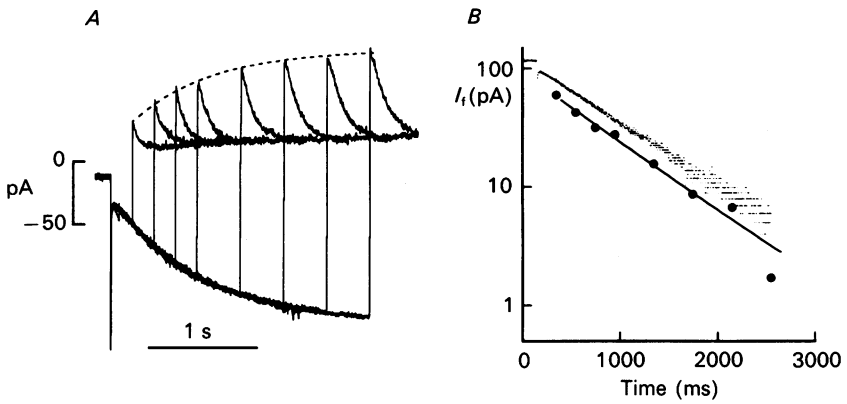

Fig. 5. Envelope of tails test. *A*, I_f tail currents were recorded at +10 mV following hyperpolarizing clamp steps to −100 mV ranging from 200 to 2400 ms in duration. Holding potential was −40 mV. Eight traces of I_f activation are superimposed. Note that the time course of the envelope curve (dashed line) of tail currents is similar to I_f activation. *B*, I_f elicited at −100 mV is plotted on a semilogarithmic scale against time and peak I_f tail current amplitudes (●) are plotted on the same scale against the duration of the preceding clamp step. The straight line was determined by least-squares analysis of the tail current amplitudes. External solution contained 3 mM-Ni^{2+}, 3 mM-Ba^{2+} and 2 mM-4-aminopyridine.

uncommon. I_f also exhibited various degrees of run-down following rupture of the membrane patch. Similar findings have been reported in SA node pacemaker cells (DiFrancesco *et al.* 1986). In five experiments, I_f decreased to 77 ± 4% of control at 10 min after breaking the membrane. To minimize run-down, most experiments were performed within 5–10 min of breaking the membrane.

Voltage dependence of I_f activation

In Fig. 4, the voltage dependence of I_f activation was determined using an experimental protocol similar to that described by DiFrancesco *et al.* (1986). The cell was hyperpolarized to various test voltages to activate I_f, and then clamped to a fixed positive voltage to elicit deactivating tail currents (Fig. 4*A*). Longer hyperpolarizing clamp pulses were used at less negative voltages where the time course of I_f activation was slower. As shown in Fig. 4*B*, the activation curve is S-shaped and shows that I_f was activated at voltages more negative than −50 mV and fully activated at about −120 mV. The half-maximal activation voltage and slope factor, calculated using a Boltzmann function, were 80·5 mV and 8·4, respectively.

To ensure correct interpretation of the I_f activation curve it is important to demonstrate that the I_f tail currents accurately reflect I_f activation. In other words, if channel conductance does not change instantaneously then the initial amplitude of the tail currents should reflect I_f activated during hyperpolarization as a function of

time. A common way of demonstrating this is to perform an 'envelope of tails' test (Giles & Shibata, 1985; DiFrancesco *et al.* 1986; van Ginneken & Giles, 1991). This was accomplished by activating I_f at a single voltage for different periods of time and then returning the membrane to a more positive fixed voltage. As shown in Fig. 5*A*,

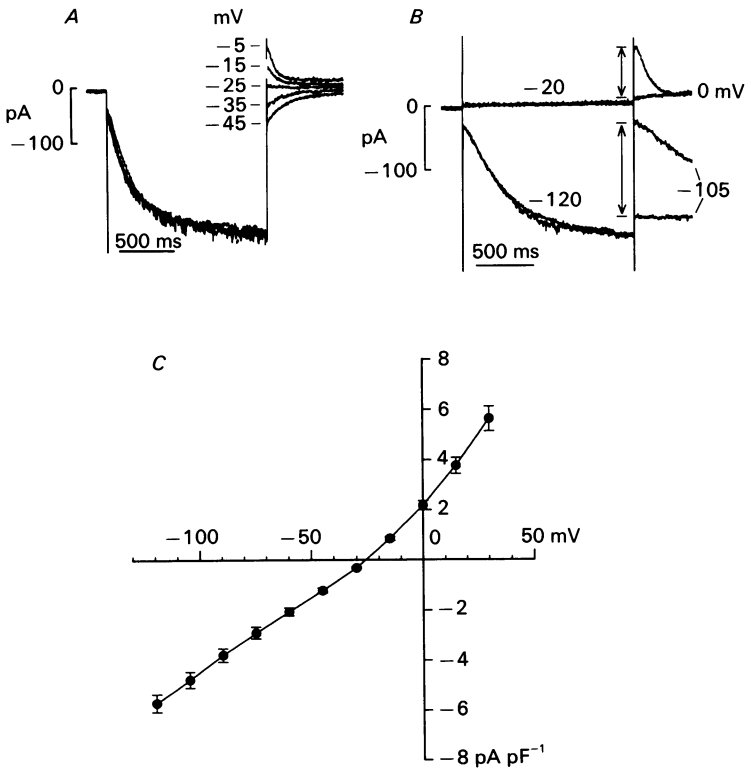

Fig. 6. *A*, determination of I_f reversal potential. From a holding potential of −40 mV, the cell was hyperpolarized to −120 for 1·5 s and then clamped to voltages between −45 and −5 mV as indicated. Five traces of I_f are superimposed. External solution contained 20 μM-TTX, 3 mM-Ni^{2+}, 3 mM-Ba^{2+} and 2 mM-4-aminopyridine. *B*, selected currents used to determine the fully activated *I–V* relationship. The cell was held at −40 mV and clamped to voltages at which the steady-state I_f activation variable (q_∞) is either 1 (−120 mV) or 0 (−20 mV), followed by clamp steps to identical voltages ranging from −105 to +30 mV. Differences between the initial tail current amplitudes (arrows) were plotted (panel *C*) against the voltages at which the tail currents were elicited. External solutions contained 3 mM-Ni^{2+}, 3 mM-Ba^{2+} and 2 mM-4-aminopyridine. *C*, fully activated *I–V* relationship for I_f determined from twenty-one cells. Currents are expressed as current density (pA pF^{-1}).

the time course of the envelope curve (dashed line) describing the peak tail currents was similar to I_f activation. In panel *B*, the I_f current shown in panel *A*, and the peak tail current amplitudes are plotted on a semilogarithmic scale as a function of time. It is apparent that the time course of both I_f activation and the envelope of tails are similar, with time constants of 808 and 737 ms, respectively. These results indicate that the peak tail currents are a reliable measure of the amount of I_f activation.

Ionic selectivity of I_f

The reversal potential of I_f was determined by hyperpolarizing the cell to activate I_f and then returning to more positive voltages in 10 mV increments. The records in Fig. 6*A* show a typical experiment where I_f tail currents reversed direction at about

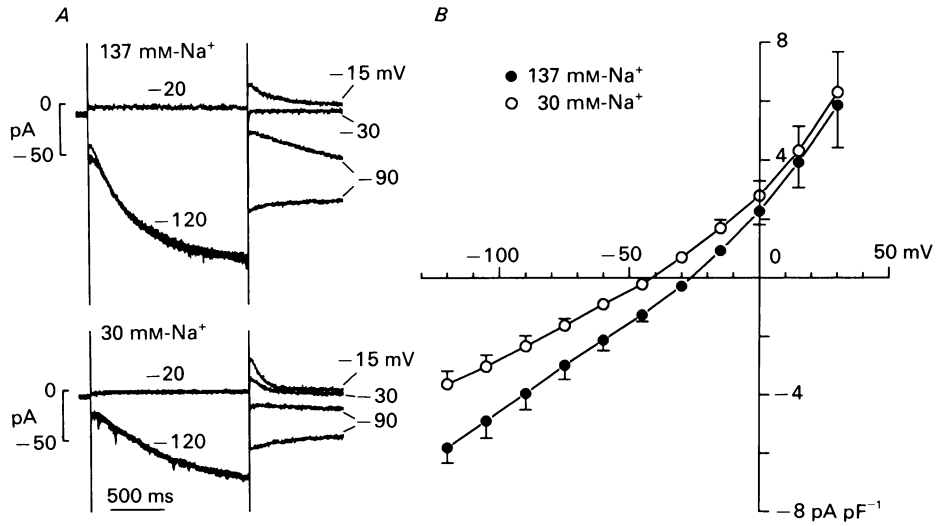

Fig. 7. Effect of low extracellular Na^+ on I_f. *A*, selected currents recorded in 137 mM-external Na^+ (top) and 30 mM-external Na^+ (bottom) solutions. Tail currents shown are those elicited from −120 to −90, −30, −15 mV and from −20 to −90 mV. *B*, fully activated *I–V* relationship in 137 mM-Na^+ (●) and 30 mM-Na^+ (○) determined in four cells. External solutions contained 3 mM-Ni^{2+}, 3 mM-Ba^{2+} and 2 mM-4-aminopyridine.

−25 mV, suggesting that I_f is carried by more than one ion species. Similar results were found in a total of ten experiments. The properties of the I_f channel were further analysed by determining the fully activated current–voltage (*I–V*) relationship, according to the method of DiFrancesco (1981*b*). In panel *C*, the fully activated *I–V* relationship is approximately linear between −120 and −30 mV, and shows outward rectification at more positive voltages. The *I–V* relationship also shows that the current changed direction at $-25{\cdot}6 \pm 0{\cdot}7$ mV ($n = 21$), which is similar to the reversal potential determined in Fig. 4*A*. Similar values have been reported for SA node pacemaker cells (DiFrancesco *et al.* 1986; van Ginneken & Giles, 1991). Measured over the linear portion of the *I–V* relationship (−30 to −120 mV) the fully activated conductance was $1{\cdot}75 \pm 0{\cdot}14$ nS ($n = 21$). This value is significantly smaller than the fully activated conductance of I_f reported in SA node (DiFrancesco *et al.* 1986; van Ginneken & Giles, 1991).

The reversal potential measurements suggest that I_f may be carried by both Na^+ and K^+ ions, as shown in other cardiac pacemaker cells (DiFrancesco, 1981*b*; Callewaert *et al.* 1984; DiFrancesco *et al.* 1986; Bois & Lenfant, 1990). This was tested by changing extracellular Na^+ or K^+ concentrations, and determining the effects on the fully activated *I–V* relationship. In Fig. 7*A*, when the extracellular Na^+

was reduced from 137 to 30 mM I_f amplitude was decreased. Panel *B* shows that reducing the external Na^+ shifted the fully activated *I–V* relationship more outward, and changed the reversal potential from $-26{\cdot}6 \pm 0{\cdot}6$ to $-41{\cdot}5 \pm 1{\cdot}6$ mV ($n = 4$). Reducing the external Na^+ also decreased the slope of the *I–V* relationship,

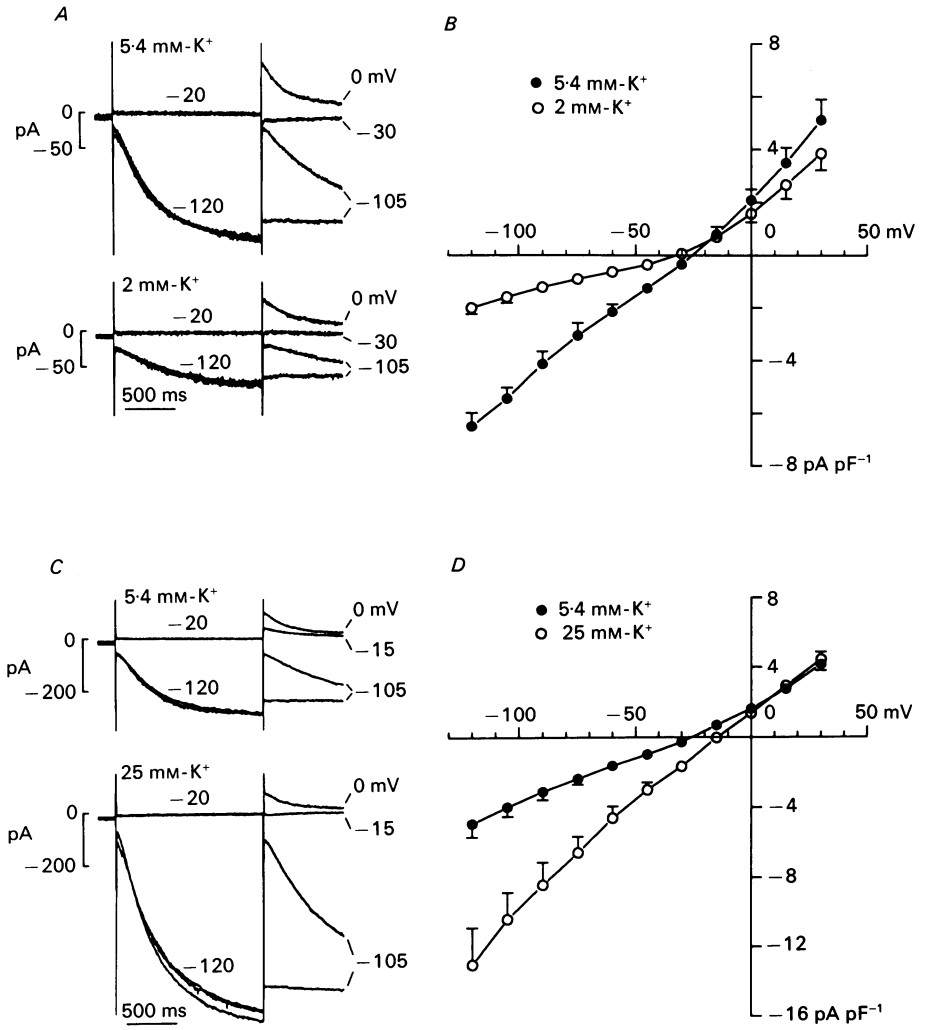

Fig. 8. Effects of different extracellular K^+ concentrations on I_f. *A*, selected currents recorded in 5·4 mM-external K^+ (top) and 2 mM-external K^+ (bottom) solutions. *B*, fully activated *I–V* relationship in 5·4 mM-K^+ (●) and 2 mM-K^+ (○) determined in four cells. *C*, selected currents recorded in 5·4 mM-external K^+ (top) and 25 mM-external K^+ (bottom) solutions. *D*, fully activated *I–V* relationship in 5·4 mM-K^+ (●) and 25 mM-K^+ (○) determined in five cells.

indicating a decrease in conductance. The change in slope is more evident at more negative voltages. At voltages more negative than about −50 mV, where the *I–V* curve is approximately linear, the reduction in external Na^+ decreased the slope by

about 25%. Others have shown that lowering external Na^+ shifts the fully activated I–V relationship to more negative voltages in Purkinje fibres (DiFrancesco, 1981*b*) and single SA node pacemaker cells (DiFrancesco *et al.* 1986). However, in contrast to the present results, those studies reported no change in the slope of the fully

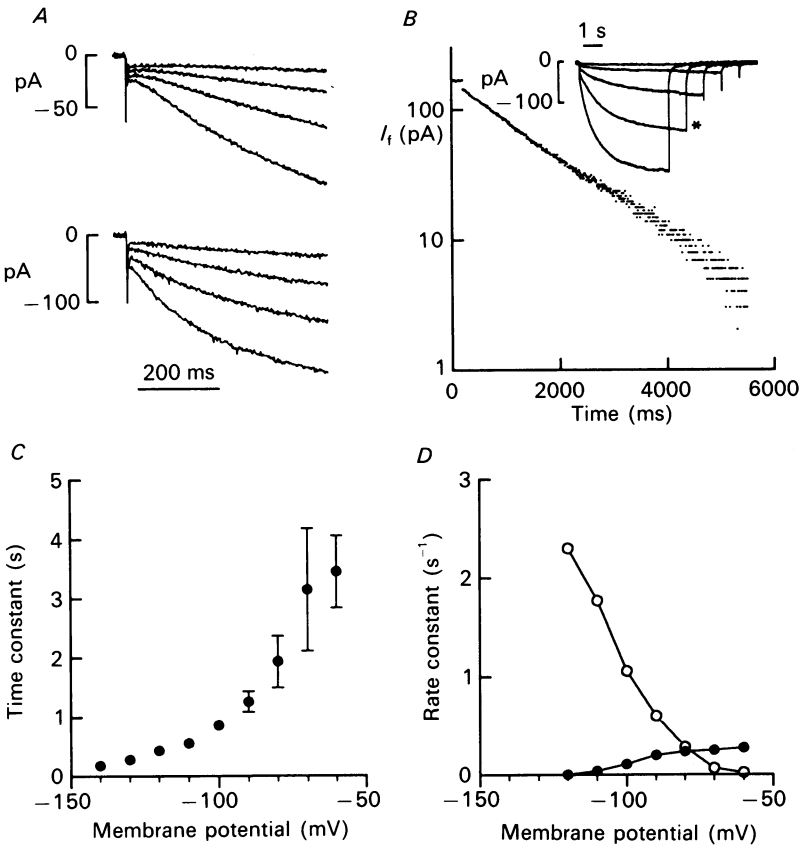

Fig. 9. Kinetic analysis of I_f. *A*, recordings of I_f from two different latent pacemaker cells showing sigmoidal time course of activation (top) and no delay in activation (bottom). Cells were held at −40 mV and hyperpolarized to voltages between −80 and −110 mV in 10 mV increments. *B*, the inset shows I_f currents exhibiting no delay in onset in a cell held at −40 mV and hyperpolarized to voltages between −60 and −100 mV in 10 mV increments for 5–9 s. The current trace at −90 mV (asterisk) was plotted on a semilogarithmic scale against time. *C*, time constants of activation at different voltages of I_f currents exhibiting single exponential time courses. Data points (●) are means ± S.E.M. obtained from four cells. *D*, rate constants α (○) and β (●) of I_f activation exhibiting single exponential time courses. Lines are drawn through data points.

activated I–V relationship with a reduction in external Na^+. Figure 8 shows the effects of lower (panels *A* and *B*) and higher (panels *C* and *D*) extracellular K^+ concentrations on I_f. In panel *A*, reducing the external K^+ from 5·4 to 2 mM decreased I_f amplitude. In panel *B*, the reversal potential of the fully activated I–V relationship was shifted from $-24{\cdot}1 \pm 3{\cdot}6$ to $-31{\cdot}2 \pm 3{\cdot}8$ mV and the slope of the I–V relationship

was decreased. The two I–V curves cross over one another at about −18 mV. As shown in panels C and D, when external K^+ was increased from 5·4 to 25 mM I_f amplitude increased, the reversal potential shifted from −25·4±0·6 to −14·7±0·7 mV, and the slope of the I–V relationship increased. These results

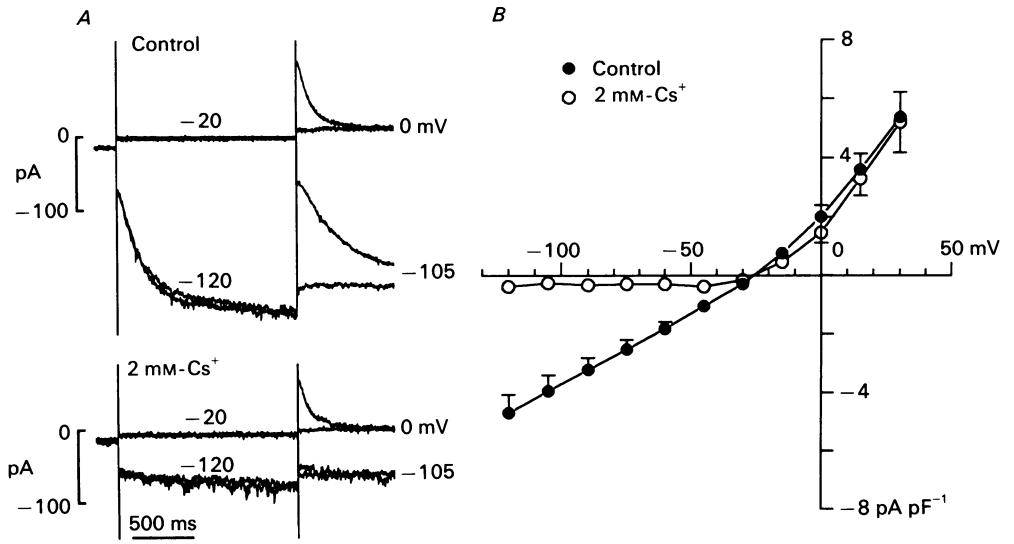

Fig. 10. Effects of Cs^+ on I_f. A, selected current recordings in control (top) and in the presence of 2 mM-Cs^+ (bottom) solutions used to determine fully activated I–V relationship (see Fig. 6). Tail currents at −105 and 0 mV were elicited from clamps to −120 and −20 mV. B, fully activated I–V relationship in control (●) and 2 mM-Cs^+ (○) determined in four cells. External solutions contained 3 mM-Ni^{2+}, 3 mM-Ba^{2+} and 2 mM-4-amino-pyridine.

indicate that K^+ is a charge carrier of I_f, similar to that reported in SA node (DiFrancesco & Ojeda, 1980; DiFrancesco *et al.* 1986) and Purkinje fibres (DiFrancesco, 1982). In addition, it has been reported that the increase in slope of the fully activated I–V relationship induced by elevated K^+ indicates that K^+ exerts an activation-like affect on I_f (DiFrancesco, 1982; DiFrancesco *et al.* 1986). The present findings indicate that I_f in latent atrial pacemaker cells is carried by both Na^+ and K^+ ions, as reported in Purkinje fibres (DiFrancesco, 1981*b*), Purkinje cells (Callewaert *et al.* 1984) and single SA node pacemaker cells (DiFrancesco *et al.* 1986).

Kinetics of I_f

Figure 9*A* shows I_f currents recorded from two different latent pacemaker cells in which activation of I_f exhibited either a short delay in onset, yielding a sigmoidal time course or little, if any, delay in onset. Similar features have been described for I_f in SA node (DiFrancesco *et al.* 1986; van Ginneken & Giles, 1991) and Purkinje cells (Callewaert *et al.* 1984). Of the seven cells studied, four cells exhibited I_f activation without delay and three cells exhibited a sigmoidal time course. I_f currents that exhibited a sigmoidal time course could not be fitted adequately with either a single exponential function or an exponential with a power of 2 (van Ginneken &

Giles, 1991). There is considerable evidence that sigmoidal I_f currents do not exhibit kinetic properties consistent with a Hodgkin–Huxley model (Hart, 1983; DiFrancesco & Ferroni, 1983; DiFrancesco, 1985). We therefore have restricted the present kinetic analysis of I_f to those currents that exhibited no delay in onset of

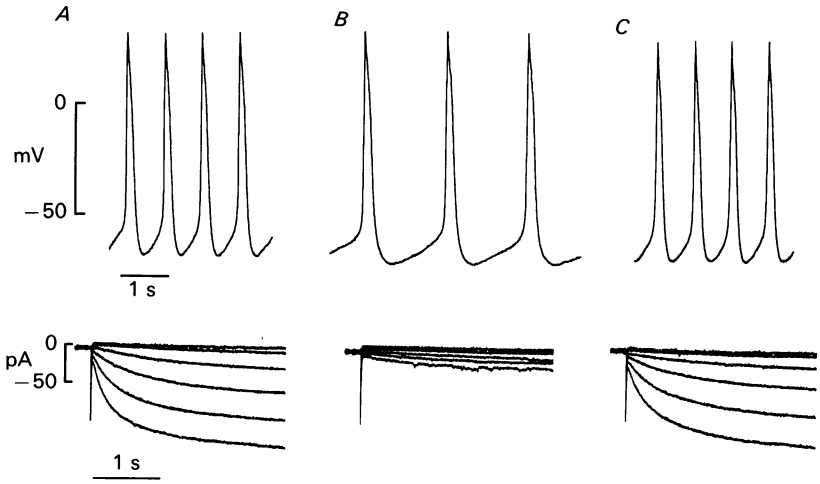

Fig. 11. Effect of Cs^+ on pacemaker action potentials and I_f recorded from a single latent pacemaker cell. *A*, control pacemaker action potentials (top) and I_f (bottom) in normal Tyrode solution. Currents were elicited by hyperpolarizing clamps between −50 and −100 mV from a holding potential of −40 mV. *B*, effect of 2 mM-Cs^+. *C*, recovery following wash-out of Cs^+.

activation and hence, were best fitted by a single exponential function. This is illustrated in Fig. 9*B* which shows a semilogarithmic plot of I_f activation. The inset in panel *B* shows I_f currents elicited by hyperpolarizing clamps to different voltages. Longer hyperpolarizing clamp durations were delivered at less negative voltages. Figure 9*C* shows the time constants of I_f activation at different voltages for the four cells that exhibited single exponential kinetics. The mean time constants were $3{\cdot}20 \pm 1{\cdot}03$ s at −70 mV and $0{\cdot}44 \pm 0{\cdot}03$ s at −120 mV. As shown in Fig. 9*D*, the forward (○) and backward (●) rate constants for the four cells were determined by the following equations:

$$\alpha = q_\infty/\tau, \tag{1}$$

$$\beta = (1-q_\infty)/\tau, \tag{2}$$

where α is forward rate constant, β is backward rate constant, τ is the activation time constant and q_∞ is the activation variable as determined by a Boltzmann function (see Fig. 4).

Effects of caesium

Low concentrations of caesium (Cs^+) are known to specifically block I_f in cardiac pacemakers (DiFrancesco, 1982; Callewaert *et al.* 1984; DiFrancesco *et al.* 1986; Hagiwara & Irisawa, 1989). Fig. 10*A* shows selected current recordings used to determine the fully activated *I–V* relationship as described above (see Fig. 6). Cs^+

blocked I_f elicited by hyperpolarizing clamp steps although it exerted only a small affect on I_f tail currents elicited by clamps more positive than about -25 mV. Cs^+ also decreased the initial background inward current elicited by hyperpolarization. The fully activated I–V relationship in panel B shows that 2 mM-Cs^+ decreased I_f to less than 10% of control at voltages more negative than the reversal potential, and had little affect on current at more positive voltages. Similar voltage-dependent block of I_f by Cs^+ has been reported in SA node (DiFrancesco *et al.* 1986; Hagiwara & Irisawa, 1989), frog sinus venosus (Bois & Lenfant, 1990) and Purkinje tissue (DiFrancesco, 1982; Callewaert *et al.* 1984).

To determine the contribution of I_f to latent atrial pacemaker activity, Cs^+ was tested on spontaneous action potentials and I_f recorded from a single pacemaker cell. This was accomplished by using a nystatin-permeabilized patch recording method (Horn & Marty, 1988). With this method we could record normal spontaneous, pacemaker action potentials and I_f for at least 30 min without discernible change in either signal. Apparently, the permeabilized patch method avoids the run-down of pacemaker activity and I_f that may result from diffusional changes in internal constituents due to rupture of the membrane patch. As shown in Fig. 11*A* hyperpolarization elicited I_f that was activated at voltages more negative than -50 mV, which is within the pacemaker potential range (-68 to -55 mV) of this cell. Moreover, these findings are similar to those obtained with the ruptured-patch whole-cell recording method used in the experiments described above (see Fig. 3). Panel B shows that 2 mM-Cs^+ decreased the slope of diastolic depolarization and significantly increased pacemaker cycle length, although spontaneous activity did not cease. Note that the diastolic slope was depressed starting from its early development. These findings are consistent with the effects of Cs^+ on multicellular pacemaker preparations (Rubenstein & Lipsius, 1989), and indicates that the contribution of I_f is already evident during the initial phase of the pacemaker potential. Cs^+ had no significant affect on other action potential parameters, although this cell exhibited a small hyperpolarization of the maximum diastolic potential. Cs^+ also significantly inhibited I_f ($< 10\%$ of control at -70 mV) activated during hyperpolarization and decreased the initial background inward current. Panel C shows that on wash-out of Cs^+ both pacemaker action potentials and I_f recovered. In eight cells tested, 2 mM-Cs increased mean cycle length from 884 ± 28 ms to 1782 ± 146 ms, which represents a $48 \pm 5\%$ decrease in spontaneous rate ($P < 0{\cdot}01$). Following wash-out of Cs^+, cycle length returned to 935 ± 40 ms. Cs^+-induced hyperpolarization of the maximum diastolic potential was variable and not statistically significant.

To determine whether the results obtained in these experiments were influenced by the recording method (Denyer & Brown, 1990*b*), we studied the effect of Cs^+ on the spontaneous beating rate of latent atrial pacemaker cells without applying a patch electrode to the cell. Instead, we determined pacemaker cycle length by measuring contractile events with a video-based edge detector. In fifteen cells tested, cycle length was 913 ± 48 ms in the absence and 1918 ± 142 ms in the presence of 2 mM-Cs^+, which corresponds to a $50 \pm 3\%$ decrease in spontaneous rate ($P < 0{\cdot}01$). Wash-out of Cs^+ returned cycle length to 961 ± 48 ms. These values are not statistically different from those obtained using the nystatin-permeabilized patch recording

method. Whether measured with or without patch electrodes, Cs^+ significantly slowed beating rate in all cells tested but did not stop spontaneous activity. These results indicate that a Cs^+-sensitive I_f current contributes significantly to latent pacemaker activity. In addition, the run-down in pacemaker activity seen with the ruptured-patch recording method cannot solely be due to run-down of I_f activation because Cs^+ block of I_f failed to stop pacemaker activity.

DISCUSSION

We have isolated latent pacemaker cells from the Eustachian ridge of cat right atrium, and analysed the properties of the pacemaker current, I_f and its contribution to latent pacemaker function. Cells isolated from the Eustachian ridge were both pacemaker and quiescent atrial cells. Latent pacemaker cells were easily distinguished and selected for study based primarily on their spontaneous activity and morphological appearance. Pacemaker cells always exhibited rhythmic beating associated with distinct contractile responses. In addition, pacemaker cells were elongated with tapered ends, had diameters of less than 10 μm, and appeared somewhat bent or crinkled, without obvious striations. These morphological characteristics are similar to those reported for SA node pacemaker cells (Denyer & Brown, 1987, 1990*a*; Belardinelli *et al.* 1988). Latent pacemaker cells did not become rounded when exposed to normal Ca^{2+} concentrations, as described in some studies of SA node (Nakayama *et al.* 1984; Hagiwara & Irisawa, 1989) and in a study of pacemaker cells isolated from tricuspid valve (Anumonwo *et al.* 1990). In addition, they were not morphologically similar to latent pacemaker cells isolated from rabbit crista terminalis (Giles & van Ginneken, 1985).

Hyperpolarization elicited I_f with little, if any, background I_{K1} current in 94% of the 213 pacemaker cells selected for study. The lack of I_{K1} was confirmed by the fact that barium had no affect on the initial inward current jump elicited by hyperpolarization. This is a common feature of both SA node (Noma, Nakayama, Kurachi & Irisawa, 1984) as well as other latent atrial pacemakers (Giles & van Ginneken, 1985; Wu *et al.* 1991). Wu *et al.* (1991) showed that in myocytes isolated from the cat right atrium, 93% of the quiescent atrial cells studied exhibited prominent I_{K1} current, whereas 94% of atrial cells that exhibited spontaneous pacemaker activity lacked I_{K1} current. Apparently, the lack of background K^+ conductance is a requirement for atrial pacemaker function. This feature would contribute to the relatively low maximum diastolic potential and high input resistance of these cells. The present findings also show that the vast majority of latent pacemaker cells in the Eustachian ridge contain I_f. Only about 6% of the cells that exhibited pacemaker activity failed to exhibit significant I_f. In this regard, Wu *et al.* (1991) have shown that the cat right atrium may contain two types of latent atrial pacemakers; those exhibiting I_f and those lacking I_f. Giles & van Ginneken (1985) have also shown that I_f is not present in latent pacemaker cells isolated from rabbit crista terminalis. The fact that such a high percentage of pacemaker cells in the Eustachian ridge exhibit I_f emphasizes the functional importance of this region. Eustachian ridge pacemaker cells also displayed passive membrane properties that are similar to those reported for SA node cells (Denyer & Brown, 1990*a*; van Ginneken & Giles, 1991). These results, therefore, suggest that latent pacemaker cells

in the Eustachian ridge are morphologically and electrophysiologically similar to SA node pacemaker cells. This idea gains further support from studies of multicellular preparations which have shown that the Eustachian ridge contains P cell types (Sherf & James, 1979; Rubenstein *et al.* 1987) that are not morphologically different from SA node P cells (Rubenstein *et al.* 1987). In addition, both Eustachian ridge (Rubenstein *et al.* 1987) and SA node (Taylor *et al.* 1978; Rubenstein *et al.* 1987) P cells have been correlated with pacemaker activity. Latent pacemaker cells also exhibited action potentials that are similar to those recorded from multicellular Eustachian ridge pacemaker preparations (Rubenstein & Lipsius, 1989). Collectively, these findings suggest that the latent pacemaker cells studied here may be P cell types similar to those in SA node.

I_f recorded from latent atrial pacemaker cells exhibits many of the properties reported for I_f in SA node (DiFrancesco *et al.* 1986; Hagiwara & Irisawa, 1989; van Ginneken & Giles, 1991), Purkinje (DiFrancesco, 1981*a*, *b*; Callewaert *et al.* 1984) and sinus venosus pacemakers (Bois & Lenfant, 1990). Thus, I_f (1) activated at voltages more negative than -50 mV, (2) was blocked by 2 mM-Cs^+, (3) exhibited a fully activated *I–V* relationship that was approximately linear at voltages more negative than -30 mV and showed outward rectification at more positive voltages, (4) exhibited a reverse potential of -26 mV, (5) was carried by both Na^+ and K^+ ions, and (6) was increased by elevated K^+ concentrations. Although many of the characteristics of I_f are similar to those reported in SA node pacemaker cells, the time course of activation in latent pacemakers was significantly slower than in SA node, e.g. at -70 mV the time constant of I_f activation was approximately 3 s while in SA node cells values closer to 1 s have been reported (Hagiwara & Irisawa, 1989; van Ginneken & Giles, 1991). In addition, the amplitude of I_f in latent pacemaker cells was significantly smaller than I_f reported in SA node pacemaker cells (DiFrancesco *et al.* 1986; van Ginneken & Giles, 1991), even when I_f current is normalized to total cell capacitance. The smaller I_f amplitude in latent pacemaker cells is reflected also in a fully activated channel conductance that is several times smaller than that reported in SA node (DiFrancesco *et al.* 1986; van Ginneken & Giles, 1991). It is well known that latent atrial pacemakers exhibit a slower spontaneous rate than primary pacemaker activity. In multicellular tissues, a direct comparison of cat SA node and Eustachian ridge pacemaker activity showed that SA node cycle length was 434 ms whereas latent pacemaker cycle length was 948 ms (Rubenstein *et al.* 1987). It should be noted that the pacemaker cycle lengths recorded from multicellular Eustachian ridge tissues (948 ms) and those recorded from single Eustachian ridge pacemakers (901 ms) are not different from one another. The relatively slow time course and small amplitude of I_f activation may be responsible, at least in part, for the relatively long cycle length of latent compared to primary pacemakers. Interestingly, the time course of I_f activation in latent atrial pacemakers is comparable to ventricular Purkinje pacemaker cells (Callewaert *et al.* 1984). It thus appears that a relatively slow time course of I_f activation may be a common feature of both atrial and ventricular latent pacemaker activities. The slower time course of I_f activation in latent atrial pacemakers may be due to a smaller opening (α) rate constant in the pacemaker voltage range (Fig. 9*D*) compared with that reported in SA node cells (Hagiwara & Irisawa, 1989).

Several lines of evidence indicate that I_f contributes importantly to right atrial

latent pacemaker function. First, I_f was activated well within the latent pacemaker voltage range (−70 to −55 mV). In addition, blocking I_f with 2 mM-Cs^+ decreased the slope of diastolic depolarization, and resulted in consistent and significant (50%) decreases in spontaneous rate, suggesting that I_f contributes significantly to initiating the pacemaker potential. An analysis of the inward current components in SA node pacemaker cells by DiFrancesco (1991) also indicates that I_f makes the largest contribution toward initiating the primary pacemaker potential. In contrast to the present results, studies in multicellular (Noma *et al.* 1983) and single SA node cell preparations (Hagiwara & Irisawa, 1989) have shown that 2 mM-Cs^+ elicited only small decreases in spontaneous rate. Van Ginneken & Giles (1991) have also reported that in single SA node cells 1 mM-Cs^+ elicited inconsistent slowing in spontaneous rate among different cells. However, Denyer & Brown (1990*b*) used recording techniques similar to those in the present study and found that in rabbit SA node cells, 2 mM-Cs^+ consistently slowed spontaneous rate by about 20–30%. The fact that Cs^+ exerted a quantitatively greater effect in latent than in SA node pacemakers suggests that I_f may contribute more to latent than to primary pacemaker function. A possible explanation for these findings is that latent pacemakers exhibit a more negative pacemaker voltage range compared to primary pacemaker cells. A similar conclusion was proposed by Anumonwo *et al.* (1990) who found that 2 mM-Cs^+ elicited a fourfold increase in cycle length of latent pacemakers isolated from tricuspid valve, which exhibited a maximum diastolic potential of about −82 mV. Van Ginneken & Giles (1991) also found that when SA node pacemaker cells were hyperpolarized by about 10 mV, Cs^+ was more effective in inhibiting spontaneous activity. In the present study, the maximum diastolic potential of latent pacemakers averaged about −68 mV. This value is more negative than those reported for SA node pacemaker cells (Nakayama *et al.* 1984; van Ginneken & Giles, 1991) and similar to those reported in SA node by others (Denyer & Brown, 1990*a*). This apparent discrepancy may be explained by a proposal of Denyer & Brown (1990*a*) that pacemaker cells isolated from the SA node may not be derived from the central nodal region, which have been shown in multicellular preparations to have a less negative maximum diastolic potential and slower upstroke velocity (Bleeker, Mackaay, Masson-Pevet, Bouman & Becker, 1980; Opthof, Dejonge, Masson-Pevet, Jongsma & Bouman, 1986). However, measurements of maximum diastolic potentials should be viewed cautiously because of differing experimental techniques and conditions among different laboratories. Recent reports have provided evidence to support the role of I_f as a pacemaker current (Denyer & Brown, 1990*b*; DiFrancesco, 1991; van Ginneken & Giles, 1991). DiFrancesco (1991) showed that in SA node cells the diastolic slope depolarizes by about 100 mV s^{-1} which requires only 0·1 pA pF^{-1} or 3 pA of inward current in a cell with a mean capacitance of 30 pF. In the present experiments, the diastolic slope of latent pacemaker cells was about 35 mV s^{-1} and cell capacitance was 28 pF. The calculated current required to elicit this response is only 0·03 pA pF^{-1} or 1 pA. Therefore, latent pacemakers require only about one-third the inward current required by the SA node. The present experiments also show that pacemaker activity continued even after I_f was significantly blocked by Cs^+. Apparently, I_f contributes significantly, but it is neither essential nor the only mechanism contributing to latent pacemaker activity. Similar findings have

been reported in multicellular Eustachian ridge preparations (Rubenstein & Lipsius, 1989), SA node pacemaker cells (Denyer & Brown, 1990*b*; van Ginneken & Giles, 1991), and tricuspid valve pacemaker cells (Anumonwo *et al.* 1990).

In summary, the present study demonstrates the isolation of Ca^{2+}-tolerant latent pacemaker cells from the Eustachian ridge of the cat right atrium. Latent pacemakers appear morphologically and electrophysiologically similar, though not identical, to pacemaker cells isolated from SA node. The main differences are that latent atrial pacemakers exhibit a longer spontaneous cycle length, a slower time course of I_f activation and a smaller I_f amplitude. Properties exhibited by I_f make it suitable as a pacemaker current, and an important component of latent pacemaker activity.

This work was supported by NIH grant HL 27652, the American Heart Association of Metropolitan Chicago and the Department of Thoracic and Cardiovascular Surgery, Loyola University Medical Center.

REFERENCES

ANUMONWO, J. M. B., DELMAR, M. & JALIFE, J. (1990). Electrophysiology of single heart cells from the rabbit tricuspid valve. *Journal of Physiology* **425**, 145–167.

BELARDINELLI, L., GILES, W. R. & WEST, A. (1988). Ionic mechanisms of adenosine actions in pacemaker cells from rabbit heart. *Journal of Physiology* **405**, 615–633.

BLEEKER, W. K., MACKAAY, A. J. C., MASSON-PEVET, M., BOUMAN, L. N. & BECKER, A. E. (1980). Functional and morphological organization of the rabbit sinus node. *Circulation Research* **46**, 11–22.

BOINEAU, J. P., SCHUESSLER, R. B., HACKEL, D. B., MILLER, C. B., BROCKUS, C. W. & WYLDS, A. C. (1980). Widespread distribution and rate differentiation of the atrial pacemaker complex. *American Journal of Physiology* **239**, H406–415.

BOIS, P. & LENFANT, J. (1990). Isolated cells of the frog sinus venosus: properties of the inward current activated during hyperpolarization. *Pflügers Archiv* **416**, 339–346.

BROWN, H. F. & DIFRANCESCO, D. (1980). Voltage-clamp investigations of membrane currents underlying pace-maker activity in rabbit sino-atrial node. *Journal of Physiology* **308**, 331–351.

CALLEWAERT, G., CARMELIET, E. & VEREECKE, J. (1984). Single cardiac Purkinje cells: general electrophysiology and voltage-clamp analysis of the pace-maker current. *Journal of Physiology* **349**, 643–661.

DENYER, J. C. & BROWN, H. F. (1987). A method for isolating rabbit sino-atrial node cells which maintains their natural shape. *Japanese Journal of Physiology* **37**, 963–965.

DENYER, J. C. & BROWN, H. F. (1990*a*). Rabbit sino-atrial node cells: isolation and electrophysiological properties. *Journal of Physiology* **428**, 405–424.

DENYER, J. C. & BROWN, H. F. (1990*b*). Pacemaking in rabbit isolated sino-atrial node cells during Cs^+ block of the hyperpolarization-activated current i_f. *Journal of Physiology* **429**, 401–409.

DIFRANCESCO, D. (1981*a*). A new interpretation of the pace-maker current in calf Purkinje fibres. *Journal of Physiology* **314**, 359–376.

DIFRANCESCO, D. (1981*b*). A study of the ionic nature of the pace-maker current in calf Purkinje fibres. *Journal of Physiology* **314**, 377–393.

DIFRANCESCO, D. (1982). Block and activation of the pace-maker channel in calf Purkinje fibres: effects of potassium, caesium and rubidium. *Journal of Physiology* **329**, 485–507.

DIFRANCESCO, D. (1985). The cardiac hyperpolarizing-activated current, i_f. Origins and developments. *Progress in Biophysics and Molecular Biology* **46**, 163–183.

DIFRANCESCO, D. (1991). The contribution of the 'pacemaker' current. (i_f) to generation of spontaneous activity in rabbit sino-atrial node myocytes. *Journal of Physiology* **434**, 23–40.

DIFRANCESCO, D. & FERRONI, A. (1983). Delayed activation of the cardiac pacemaker current and its dependence on conditioning pre-hyperpolarizations. *Pflügers Archiv* **396**, 265–267.

DiFrancesco, D., Ferroni, A., Mazzanti, M. & Tromba, C. (1986). Properties of the hyperpolarizing-activated structure (i_f) in cells isolated from the rabbit sino-atrial node. *Journal of Physiology* **377**, 61–88.

DiFrancesco, D. & Ojeda, C. (1980). Properties of the current i_f in the sino-atrial node of the rabbit compared with those of the current i_{K2} in Purkinje fibres. *Journal of Physiology* **308**, 353–367.

Euler, D. E., Jones, S. B., Gunnar, W. P., Loeb, J. M., Murdock, D. K. & Randall, W. C. (1979). Cardiac arrhythmias in the conscious dog after excision of the sinoatrial node and crista terminalis. *Circulation* **59**, 468–475.

Giles, W. R. & Shibata, E. F. (1985). Voltage clamp of bull-frog cardiac pace-maker cells: a quantitative analysis of potassium currents. *Journal of Physiology* **368**, 265–292.

Giles, W. R. & van Ginneken, A. C. G. (1985). A transient outward current in isolated cells from the crista terminalis of rabbit heart. *Journal of Physiology* **368**, 243–264.

Glitsch, H. G., Pusch, H., Schumacher, T. & Verdonck, F. (1982). An identification of the K activated Na pump current in sheep Purkinje fibers. *Pflügers Archiv* **394**, 256–263.

Hagiwara, N. & Irisawa, H. (1989). Modulation by intracellular Ca^{2+} of the hyperpolarization-activated inward current in rabbit single sino-atrial node cells. *Journal of Physiology* **409**, 121–141.

Hamill, O. P. Marty, A., Neher, E., Sakmann, B. & Sigworth, F. J. (1981). Improved patch-clamp techniques for high resolution current recording from cells and cell-free membrane patches. *Pflügers Archiv* **391**, 85–100.

Hart, G. (1983). The kinetics and temperature dependence of the pace-maker current i_f in sheep Purkinje fibres. *Journal of Physiology* **337**, 401–416.

Horn, R. & Marty, A. (1988). Muscarinic activation of ionic currents measured by a new whole-cell recording method. *Journal of General Physiology* **92**, 145–159.

James, T. N., Sherf, L., Fine, G. & Morales, A. R. (1966). Comparative ultrastructure of the sinus node in man and dog. *Circulation* **34**, 139–163.

Jones, S. B., Euler, D. E., Hardie, E., Randall, W. C. & Brynjolfsson, G. (1978). Comparison of SA nodal and subsidiary atrial pacemaker function and location in the dog. *American Journal of Physiology* **234**, H471–476.

Kenyon, J. L. & Gibbons, W. R. (1979). 4-Aminopyridine and the early outward current of sheep cardiac Purkinje fibers. *Journal of General Physiology* **73**, 139–157.

Kimura, J., Miyamae, S. & Noma, A. (1987). Identification of sodium–calcium exchange current in single ventricular cells of guinea-pig. *Journal of Physiology* **384**, 199–222.

Nakayama, T., Kurachi, Y., Noma, A. & Irisawa, H. (1984). Action potential and membrane currents of single pacemaker cells of the rabbit heart. *Pflügers Archiv* **402**, 248–257.

Nathan, R. D. (1986). Two electrophysiologically distinct types of cultured pacemaker cells from rabbit sinoatrial node. *American Journal of Physiology* **250**, H325–329.

Noble, D. (1985). Ionic basis of rhythmic activity in the heart. In *Cardiac Electrophysiology and Arrhythmias*, ed. Zipes, D. & Jalife, J., pp. 3–11. Grune & Stratton Inc., FL, USA.

Noma, A., Morad, M. & Irisawa, H. (1983). Does the 'pacemaker current' generate the diastolic depolarization in the rabbit s.a. node cells? *Pflügers Archiv* **397**, 190–194.

Noma, A., Nakayama, T., Kurachi, Y. & Irisawa, H. (1984). Resting K conductance in pacemaker and non-pacemaker heart cells of the rabbit. *Japanese Journal of Physiology* **34**, 245–254.

Opthof, T., Dejonge, B., Masson-Pevet, M., Jongsma, H. J. & Bouman, L. N. (1986). Functional and morphological organization of the cat sinoatrial node. *Journal of Molecular and Cellular Cardiology* **18**, 1015–1031.

Osterrieder, W., Yang, Q.-F. & Trautwein, W. (1982). Effects of barium on the membrane current in the rabbit S-A node. *Pflügers Archiv* **394**, 78–84.

Randall, W. C., Talano, J., Kaye, M. P., Euler, D. E., Jones, S. B. & Brynjolfsson, G. (1978). Cardiac pacemakers in the absence of the SA node: responses to exercise and autonomic blockade. *American Journal of Physiology* **234**, H465–470.

Rozanski, G. J. & Lipsius, S. L. (1985). Electrophysiology of functional subsidiary pacemakers in canine right atrium. *American Journal of Physiology* **249**, H594–603.

Rozanski, G. J., Lipsius, S. L. & Randall, W. C. (1983). Functional characteristics of sinoatrial and subsidiary pacemaker activity in the canine right atrium. *Circulation* **67**, 1378–1387.

RUBENSTEIN, D. S., FOX, L. M., MCNULTY, J. A. & LIPSIUS, S. L. (1987). Electrophysiology and ultrastructure of Eustachian ridge from cat right atrium: a comparison with SA node. *Journal of Molecular and Cellular Cardiology* **19**, 965–976.

RUBENSTEIN, D. S. & LIPSIUS, S. L. (1989). Mechanisms of automaticity in subsidiary pacemakers from cat right atrium. *Circulation Research* **64**, 648–657.

SEALY, W. C., BACHE, R. J., SEABER, A. V. & BHATTACHARGA, S. K. (1973). The atrial pacemaking site after surgical exclusion of the sinoatrial node. *Journal of Thoracic and Cardiovascular Surgery* **65**, 841–850.

SHERF, L. & JAMES, T. N. (1979). Fine structure of cells and their histologic organization within internodal pathways of the heart: Clinical and electrocardiographic implications. *American Journal of Cardiology* **44**, 345–369.

TAYLOR, J. J., D'AGROSA, L. S. & BURNS, E. M. (1978). The pacemaker cell of the sinoatrial node of the rabbit. *American Journal of Physiology* **235**, H407–412.

VAN GINNEKEN, A. C. G. & GILES, W. (1991). Voltage clamp measurements of the hyperpolarization-activated inward current I_f in single cells from rabbit sino-atrial node. *Journal of Physiology* **434**, 57–83.

WU, J., VEREECKE, J., CARMELIET, E. & LIPSIUS, S. L. (1991). Ionic currents activated during hyperpolarization of single right atrial myocytes from cat heart. *Circulation Research* **68**, 1059–1069.

YANAGIHARA, K. & IRISAWA, H. (1980). Inward current activated during hyperpolarization in the rabbit sinoatrial node cell. *Pflügers Archiv* **385**, 11–19.

ZHOU, Z. & LIPSIUS, S. L. (1990). Ionic current mechanisms of latent atrial pacemakers (abstract). *Circulation* **82**, 526.